

Ff Gene 5 Protein Has a High Binding Affinity for Single-Stranded Phosphorothioate DNA[†]

Tung-Chung Mou,[‡] Carla W. Gray,[‡] Thomas C. Terwilliger,[§] and Donald M. Gray^{*,‡}

Department of Molecular and Cell Biology, The University of Texas at Dallas, Box 830688, Richardson, Texas 75083-0688, and Life Sciences Division, MS M888, Los Alamos National Laboratory, Los Alamos, New Mexico 87545

Received September 11, 2000; Revised Manuscript Received December 19, 2000

ABSTRACT: The gene 5 protein (g5p) of Ff bacteriophages is a well-studied model ssDNA-binding protein that binds cooperatively to the Ff ssDNA genome and single-stranded polynucleotides. Its affinity, $K\omega$ (the intrinsic binding constant times a cooperativity factor), can differ by several orders of magnitude for ssDNAs of different nearest-neighbor base compositions [Mou, T. C., Gray, C. W., and Gray, D. M. (1999) *Biophys. J.* 76, 1537–1551]. We found that the DNA backbone can also dramatically affect the binding affinity. The $K\omega$ for binding phosphorothioate-modified S-d(A)₃₆ was >300-fold higher than for binding unmodified P-d(A)₃₆ at 0.2 M NaCl. CD titrations showed that g5p bound phosphorothioate-modified oligomers with the same stoichiometry as unmodified oligomers. The CD spectrum of S-d(A)₃₆ underwent the same qualitative change upon protein binding as did the spectrum of unmodified DNA, and the phosphorothioate-modified DNA appeared to bind in the normal g5p binding site. Oligomers of d(A)₃₆ with different proportions of phosphorothioate nucleotides had binding affinities and CD perturbations intermediate to those of the fully modified and unmodified sequences. The influence of phosphorothioation on binding affinity was nearly proportional to the extent of the modification, with a small nearest-neighbor dependence. These and other results using d(ACC)₁₂ oligomers and mutant proteins indicated that the increased binding affinity of g5p for phosphorothioate DNA was not a polyelectrolyte effect and probably was not an effect due to the altered nucleic acid structure, but was more likely a general effect of the properties of the sulfur in the context of the phosphorothioate group.

One of the most frequently employed modifications of antisense DNA oligomers is phosphorothioation. Phosphorothioate DNA (S-DNA)¹ differs from normal DNA (P-DNA) in having one of the nonbridging backbone oxygens of each phosphodiester replaced with sulfur. S-DNA retains the net backbone negative charge, ability to activate RNase H, and solubility in aqueous solvents of P-DNA, and it has the advantages of higher nuclease resistance and increased cellular uptake relative to DNA with normal phosphodiester linkages (1–3).

The basis of antisense drug therapy with phosphorothioates is that single-stranded S-DNA oligomers can form a sequence-specific hybrid duplex with target mRNA sequences whose translation is then disrupted by RNase H cleavage of the

mRNA strand. However, S-DNAs also bind to cellular single-stranded nucleic acid binding proteins and to proteins involved in cell growth, viral proliferation, enzymatic activity, and cellular adhesion (1, 4–11). The binding of S-DNAs to serum albumin has been correlated with the percentage of phosphorothioate content (4).

In the design of an optimal antisense oligonucleotide it is desirable to reduce the nonsequence-specific interactions between the antisense oligonucleotide and proteins. Unfortunately, the nature of nonspecific interactions between S-DNA and proteins is still not clear because the sulfur substitution can influence binding in a number of ways, whose relative importance depends on the particular nucleic acid and protein being studied. In this present work, we used the Ff g5p as a model protein to investigate the nonspecific binding of S-DNA. The Ff g5p is a small (87 amino acids), dimeric single-stranded nucleic acid binding protein, which plays an essential role in the life cycles of Ff filamentous bacterial viruses. In the absence of nucleic acid, the dimeric structure of g5p has been determined by X-ray crystallography and NMR spectroscopy (12, 13). The structure of the g5p-ssDNA complex, which forms a left-handed superhelix, has been studied by electron microscopy, NMR and CD spectroscopy, solution scattering techniques, and molecular modeling (12, 14–17). The binding properties of g5p have similarities to those of other single-stranded nucleic acid binding proteins, such as T4 g32p, *Escherichia coli* SSB, and human replication protein A (RPA), in the conservation

[†] This work was performed by T.-C. M. in partial fulfillment of the requirements for the Ph.D. degree in the Department of Molecular and Cell Biology, The University of Texas at Dallas. This work was supported by grants from the Robert A. Welch Foundation (AT-503), the Texas Advanced Technology Program (009741-0021-1999), and Cytoclonal Pharmaceuticals, Inc. (Dallas, TX) to D.M.G., and by NIH Grant RO1 38714 to T.C.T.

^{*} To whom correspondence should be addressed. Phone: (972) 883-2513. Fax: (972) 883-2409. E-mail: dongray@utdallas.edu.

[‡] The University of Texas at Dallas.

[§] Los Alamos National Laboratory.

¹ Abbreviations: CD, circular dichroism; Ff, filamentous phages (M13, fd, and f1) that require F pili to infect *E. coli*; g5p, gene 5 protein; $K\omega$, the intrinsic binding constant K times a cooperativity factor ω ; [P]/[N], [protein monomer]/[nucleotide] molar ratio; P-DNA, DNA with normal phosphodiester linkages; S-DNA, DNA with phosphorothioate-modified linkages; ssDNA, single-stranded DNA.

of aromatic residues in the binding site and in having an electrostatic component of interaction with the nucleic acid (12, 18–20). NMR and mutagenesis studies suggest that the g5p–ssDNA interactions involve stacking of the nucleic acid bases with the aromatic rings of Tyr-26 and Phe-73 in or very near the g5p DNA binding loop and electrostatic interactions between the nucleic acid phosphodiester bond and Lys-24, Lys-46, and Lys-69 (12, 16, 17, 21–24). Since g5p binds cooperatively to the entire single-stranded virus genome, with a stoichiometry of four nucleotides per g5p monomer, the g5p is considered to be a nonsequence-specific binding protein. However, the binding affinities of g5p vary greatly for ssDNAs that have simple sequences (25), and the binding affinities to various (A+C)-containing sequences are related to the nearest-neighbor base composition (26).

We used CD measurements to investigate differences in the characteristics of binding of wild-type and mutant Ff gene 5 proteins to single-stranded d(A)₃₆ and d(AAC)₁₂ with phosphodiester or phosphorothioate linkages. The results demonstrated that, with the same binding stoichiometry, g5p has a dramatically higher binding affinity for S-DNA than for P-DNA. The effect of phosphorothioation on g5p binding affinity was largely independent of the type of protein mutant or which sequence was modified.

MATERIALS AND METHODS

Protein and Oligonucleotides. Wild-type Ff gene 5 protein was isolated from *E. coli* K561 cells containing a plasmid encoding the g5p gene as previously described (27–29). The protein was over 99% pure by electrophoresis on 18% polyacrylamide gels. Protein concentrations were determined from absorption measurements using molar extinction coefficients $\epsilon(276)$ of 7074 and 5660 M⁻¹ cm⁻¹ for the wild-type and mutant proteins, respectively (28). The protein was finally dialyzed into 2 mM Na⁺ (phosphate buffer, pH 7.0).

The DNA oligomers used in this study were all 36 nucleotides long. Adenosine oligomers with phosphodiester linkages, P-dA₃₆, and with phosphorothioate linkages, S-dA₃₆, were purchased from Oligos, Etc. (Wilsonville, OR). Three chimeric phosphodiester/phosphorothioate dA₃₆ oligonucleotides and two mixed-base sequences [P-d(AAC)₁₂ and S-d(AAC)₁₂] were purchased from Midland Certified Reagent Co. (Midland, TX). Two of the chimeric sequences were sequences with repeating phosphate and phosphorothioate linkages, d[Ap(AsApApAp)₈AsApA] and d[Ap(AsAsApAp)₈AsAsA]; they will be denoted SPPP-dA₃₆ and SSPP-dA₃₆, respectively. SPPP-dA₃₆ and SSPP-dA₃₆ had one or two phosphorothioate linkages every four adenosine residues and therefore had about 26 and 51% phosphorothioate linkages, respectively, of the 35 total linkages. (There were no phosphates at either end of the oligomers.) The third chimeric sequence was a nonrepeating 36-mer, (As)₂Ap(As)Ap(As)₆Ap(As)Ap(As)₄Ap(As)Ap(As)₆Ap(As)₂Ap(As)₂Ap(As)A, having 26 (about 74%) phosphorothioate linkages and will be denoted (S₃P)-dA₃₆. P-dA₃₆ and S-dA₃₆ were gel purified, and electrophoresis on 12% polyacrylamide sizing gels (by Oligos, Etc.) showed no detectable postsynthesis fragmentation due to depurination (at a detection limit of <2% for a given size fragment). The chimeric oligomers were purified by HPLC, and mass spectroscopy (by Midland) showed no detectable fragmentation. The oligomers were all

provided as lyophilized ammonium salts and were directly dissolved in 2 mM Na⁺ (phosphate buffer, pH 7.0) for the experiments.

Concentrations of oligomers were determined from absorption spectra, using nearest-neighbor calculated $\epsilon(260)$ values of 12 050 M⁻¹ cm⁻¹ (for all five A-containing oligomers) and 10 610 M⁻¹ cm⁻¹ for the two mixed-base sequences (30). It was assumed that extinction coefficients for phosphorothioate-modified oligonucleotides were the same as for unmodified oligonucleotides. Murphy and Trapane (31) showed by phosphate analysis that nearest-neighbor calculations are no less accurate for phosphorothioate DNAs than for unmodified DNAs.

CD Titrations. CD spectra were acquired as described by Mou et al. (26). Smoothed CD spectra were plotted at 1-nm intervals as $\epsilon_L - \epsilon_R$ (M⁻¹ cm⁻¹ per mol of nucleotide). Titrations were performed by adding aliquots of concentrated g5p ($\sim 1 \times 10^{-4}$ M) to the oligomers in 2 mM Na⁺ (phosphate buffer, pH 7.0). The volume of the added g5p and the dilution of the oligonucleotide were calculated by weighing the sample before and after each addition. The sample was gently mixed and allowed to reach equilibrium. Final nucleotide concentrations were $4\text{--}6 \times 10^{-5}$ M in the titrated samples. Light scattering was measured by monitoring the UV absorption at ≥ 320 nm; at the highest [P]/[N] ratios, the absorption at 320 nm was at most 5.5% of the absorption at 260 nm of the free oligonucleotide before the titration.

Salt Dissociation and Binding Affinity. Saturated protein–DNA complexes were formed at [P]/[N] = 0.25 in 2 mM Na⁺ (phosphate buffer, pH 7.0). Salt dissociations of the complexes were performed as in previous work (26). The percent dissociation of a nucleic acid from a g5p complex was monitored by CD measurements at 263 or 270 nm and plotted as a function of [NaCl]. The salt concentration required for 50% dissociation was determined from the dissociation curve. As in previous work, the salt dissociation curve was shown to be consistent with all-or-none binding to a finite lattice (26). Hence, apparent values of the binding constant product $K\omega_{\text{app}}$ per dimer were derived with the assumption that the dissociation was all-or-none by setting $K\omega_{\text{app}} = 1/(2L)$, where L was the free dimer concentration at 50% dissociation. These $K\omega_{\text{app}}$ values are those described by Terwilliger (32) for the simultaneous binding model, but are divided by two to correct for the 2-fold symmetry of the g5p (29). This yields the $K\omega_{\text{app}}$ for binding of the g5p dimer in one orientation to two DNA strands (29, 32, 33). These are called apparent values since they differ from the $K\omega$ values that would be determined for binding within an infinite lattice.

Zeroth-Neighbor and Nearest-Neighbor Binding Dependencies from Singular Value Decomposition. Two models were used to describe the dependence of binding affinity on the occurrence of phosphorothioate linkages in P-dA₃₆, S-dA₃₆, and the three chimeric oligomers. In the first model, called the “zeroth-neighbor” model, the $\log[K\omega_{\text{app}}]$ values for binding of g5p to the five synthetic dA₃₆ oligonucleotides were considered to be the weighted sums of two $\log[K\omega_{\text{app}}]$ parameters that describe the binding to phosphodiester and phosphorothioate linkages. For the second model, called the “nearest-neighbor” model, the $\log[K\omega_{\text{app}}]$ values for binding of g5p to the five dA₃₆ oligonucleotides were considered to be the weighted sums of three $\log[K\omega_{\text{app}}]$ parameters that

describe the binding to three simple combinations of phosphodiester and phosphorothioate linkages. These combinations were (ApAp), (AsAs), and the average of (AsAp+ApAs). Specifically,

$$\log[K\omega_{\text{app}}(\text{synthesized sequence})]_i = \sum_j F_j \log[K\omega_{\text{app}}(\text{parameter } j)] \quad (1)$$

where F_j is the fraction of linkage or nearest-neighbor sequence parameter j in the synthesized sequence i . From the dependence of $\log[K\omega]$ on $\log[\text{NaCl}]$, the experimental $K\omega$ values per g5p dimer were extrapolated to 0.2 M NaCl for all five sequences. For zeroth-neighbor binding, the binding depends on the fractions of phosphodiester and phosphorothioate linkages and on two independent sequences with parameters, $K\omega_{\text{Ap}}$ and $K\omega_{\text{As}}$. For nearest-neighbor binding, the binding depends on the fractions of neighboring linkages and on three independent sequences with parameters, $K\omega_{\text{ApAp}}$, $K\omega_{\text{AsAs}}$, and $K\omega_{\text{AsAp+ApAs}}$. It was assumed that the 3' ends of P-dA₃₆, SPPP-dA₃₆, and SSPP-dA₃₆ had a phosphate group and that the 3' ends of S-dA₃₆ and (S₃,P)-dA₃₆ had a phosphorothioate group. It was also assumed that there were 36 nearest-neighbors for each 36-mer. That is, the sequences were considered to be closed with no ends, which amounts to neglecting 1/36 part of any differences between their binding affinities. Details of such models have been discussed (26, 34). It is relevant to note that, if the cooperativity factor, ω , is the same for binding to sequences that are all of the same length, ω cancels in eq 1 and binding affinities will depend only on the intrinsic binding factor, K .

Thus, for these models, matrix equations expressed the measured $\log[K\omega_{\text{app}}]$ values for the five synthesized oligomers (i) in terms of two or three parameters (j) as follows: $\log[K\omega_{\text{app}}]_i = F_{ij} \log[K\omega]_j$, where F_{ij} are the fractions of j th independent parameters in the i th oligonucleotide. For the best least-squares fits of $\log[K\omega_{\text{app}}]_i$ values, the $i \times j$ matrix of F_{ij}/σ_i , where σ_i is the standard deviation on $\log[K\omega_{\text{app}}]_i$ from the linear regression of $\log[K\omega_{\text{app}}]_i$ versus $\log[\text{NaCl}]$, was decomposed by singular value decomposition (SVD). Standard procedures allow each set of equations to be solved for the two zeroth-neighbor or three nearest-neighbor parameters (26, 35, 36).

Error Analysis. Errors (σ) on the measured and calculated $K\omega$ were derived as explained by Mou et al. (26). A statistical test of the SVD results for fitting the models was given by the probability (Q) that χ^2 (where $\chi^2 = \sum_i |(\log[K\omega_{\text{meas}}]_i - \log[K\omega_{\text{calc}}]_i)/\sigma_i|^2$) from a fit to the data would be larger by chance. A larger Q indicates a better fit, and Q may be acceptable above 0.001 (35).

RESULTS

CD Titrations and Binding Stoichiometries of dA₃₆ Oligomers with g5p. Five dA₃₆ oligonucleotides that differed only in their phosphorothioate contents were titrated with wild-type Ff gene 5 protein in a buffer of 2 mM Na⁺ (phosphate), pH 7.0, at 20 °C. In this buffer, the CD spectra of all five nucleic acids had small positive bands at wavelengths above 260 nm and a significant negative band at 250 nm, showing that the oligomers were single-stranded (37). Spectra of P-dA₃₆ and S-dA₃₆ are shown in Figure 1.

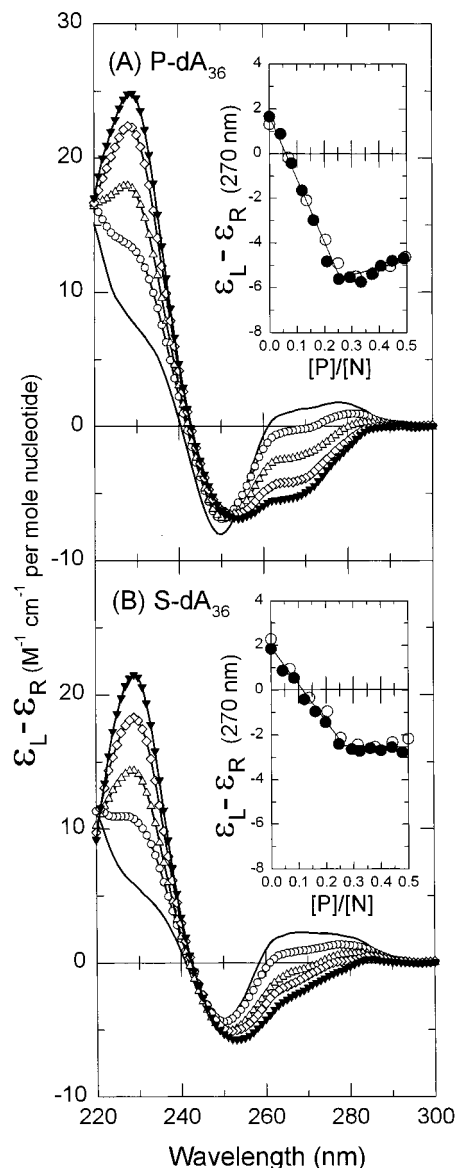


FIGURE 1: Representative CD spectra during titrations of dA₃₆ oligonucleotides with g5p. (A) CD spectra of free P-dA₃₆ (—) and g5p-P-dA₃₆ complexes at [P]/[N] ratios of 0.07 (○), 0.14 (△), 0.20 (◇), and 0.25 (▼); (B) CD spectra of free S-dA₃₆ (—) and g5p-S-dA₃₆ complexes at [P]/[N] ratios of 0.07 (○), 0.14 (△), 0.21 (◇), and 0.25 (▼). Insets show CD titration data at 270 nm as a function of [P]/[N] ratio. Different symbols are data from separate titrations. CD data are plotted as $\epsilon_L - \epsilon_R$ (M⁻¹ cm⁻¹ per mol of nucleotide).

Figure 1 shows representative spectra from CD titrations of P-dA₃₆ and S-dA₃₆ with g5p. Upon addition of g5p, the positive CD bands of the oligomers above 250 nm decreased in magnitude and became negative. The CD contribution of g5p is negligible in this wavelength range. [The largest peak above 250 nm in the CD spectrum of g5p is at 282 nm, with a magnitude of +0.7 M⁻¹ cm⁻¹/mol of g5p monomer (29). Moreover, the spectra in Figure 1 are scaled per mole of nucleotide, and the contribution of g5p to a given spectrum is proportionately reduced by the [P]/[N] ratio.] Therefore, the spectral changes at long wavelengths in Figure 1 can be assigned to alterations in the environment of the DNA nucleotides. These alterations of the nucleic acid CD spectra included effects of dehydration, unstacking, and the conformational changes needed to trace a left-handed superhelical path when complexed with g5p (14, 17, 29, 38). At short

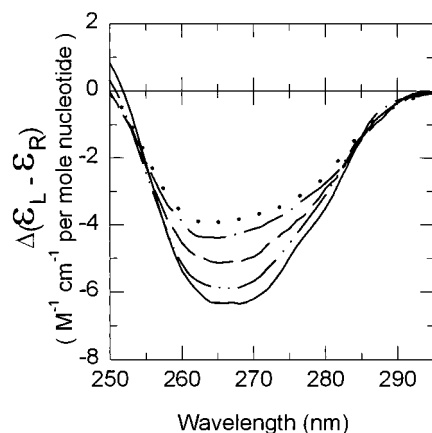


FIGURE 2: CD difference spectra calculated as the CD spectra of saturated g5p·dA₃₆ complexes minus the CD spectra of free dA₃₆ oligonucleotides. The complexes were formed between g5p and P-dA₃₆ (—), SPPP-dA₃₆ (—•—), SSPP-dA₃₆ (---), (S₃, P)-dA₃₆ (—•—), and S-dA₃₆ (•••) oligonucleotide sequences at [P]/[N] = 0.25. The free oligomers all had similar CD magnitudes above 250 nm, so the differences show that oligomers with increased phosphorothioate content were less perturbed within the g5p binding site as the phosphorothioate content increased. CD data are plotted as $\Delta(\epsilon_L - \epsilon_R)$ ($M^{-1} \text{ cm}^{-1}$ per mol of nucleotide).

wavelengths, the positive CD band below 240 nm increased during titrations with g5p because the protein does have a large positive tyrosyl CD band at 229 nm (29).

The long-wavelength CD effects of titrations of SPPP-dA₃₆, SSPP-dA₃₆, and (S₃,P)-dA₃₆ with g5p were qualitatively the same as shown in Figure 1 for titrations of P-dA₃₆ and S-dA₃₆. However, the magnitudes of CD changes were quantitatively less as the proportion of phosphorothioate linkages increased, as documented by the difference spectra in Figure 2.

The insets of Figure 1 display the long-wavelength nucleic acid CD values at 270 nm of titrated P-dA₃₆ and S-dA₃₆ as a function of the [P]/[N] ratio. Binding of g5p to P-dA₃₆ and S-dA₃₆ was essentially stoichiometric and proportional to the addition of protein until titration endpoints were reached at [P]/[N] molar ratios of 0.25 ± 0.01 , which indicated an $n = 4$ binding mode (i.e., one g5p monomer binding four nucleotides). The same titration endpoint ([P]/[N] = $0.25\text{--}0.26 \pm 0.01$) was observed for the five dA₃₆ oligomers having different combinations of phosphodiester and phosphorothioate linkages. At saturation in an $n = 4$ binding mode, there would be nine g5p dimers complexed with two dA₃₆ oligomer strands, which would be held in antiparallel binding channels of the superhelical array (17).

The identical stoichiometries of binding, as well as the similar qualitative CD changes upon binding, were evidence that all of the dA₃₆ oligomers bind to the same g5p sites.

Salt Dissociations. Salt dissociation data for complexes formed between g5p and different oligomers were obtained by monitoring the nucleic acid CD changes as the NaCl concentration was increased. Complexes were initially formed at a [P]/[N] ratio of 0.25 in 2 mM Na⁺ (phosphate), pH 7.0. As the NaCl concentration was increased, the complexes dissociated and the CD spectra above 260 nm were restored to have the positive values of the respective free oligonucleotides at a relatively high salt concentration (ref 26; and data not shown). CD changes at both 263 and 270 nm were used to monitor the fraction of dissociation.

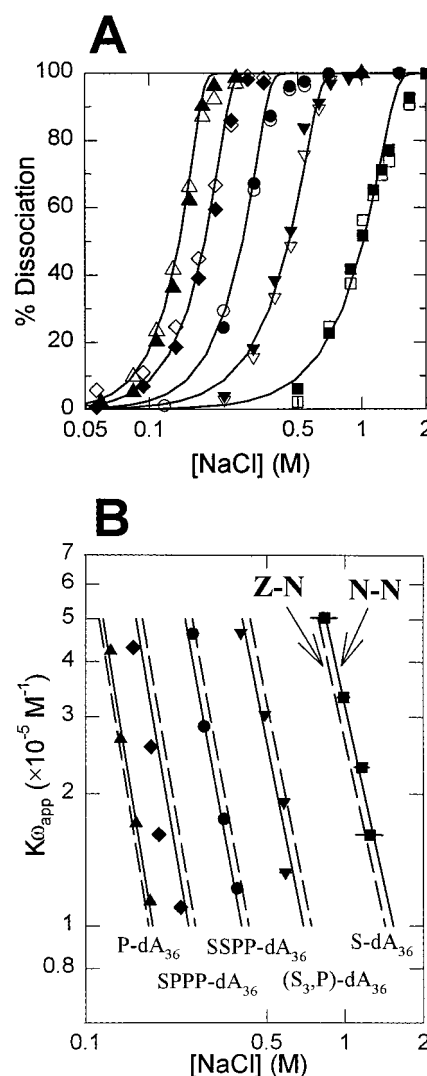


FIGURE 3: (A) Representative salt dissociation curves of complexes formed between g5p and different oligonucleotides all at [P]/[N] = 0.25. CD values were monitored at 263 nm (closed symbols) and 270 nm (open symbols). Dissociation profiles are shown of complexes with P-dA₃₆ (▲), SPPP-dA₃₆ (◆), SSPP-dA₃₆ (●), (S₃,P)-dA₃₆ (▼), and S-dA₃₆ (■). The total g5p concentrations in these samples were similar, within the range of 7.7 to 8.5 μM . The lines (—) were calculated by fitting the data points with a function as described in Mou et al. (26) for the all-or-none dissociation from finite lattices. (B) Dependence of the $\log[K\omega]$ on $\log[\text{NaCl}]$ for binding of g5p to different dA₃₆ sequences: P-dA₃₆ (▲), SPPP-dA₃₆ (◆), SSPP-dA₃₆ (●), (S₃,P)-dA₃₆ (▼), and S-dA₃₆ (■). To compare the binding affinities for these different sequences, singular value decomposition (SVD) was used to fit to data from all five dA₃₆ sequences using zeroth-neighbor (—) and nearest-neighbor (---) models. Error bars from the standard deviations in [NaCl] needed for 50% dissociation were generally within the size of the symbols shown.

Spectral changes were maximal at about 270 nm, but the CD spectra of the isolated 36-mers had little or no sensitivity to salt concentration at 263 nm.

Examples of salt dissociation profiles for the five g5p·dA₃₆ complexes are shown in Figure 3A for samples with similar total g5p concentrations (7.7–8.5 μM). The salt concentration needed for dissociation increased as the proportion of phosphorothioate linkages increased. Stabilities of complexes with the five oligomers increased as the fraction of phosphorothioate linkages increased, in the order of P-dA₃₆ < SPPP-dA₃₆ < SSPP-dA₃₆ < (S₃,P)-dA₃₆ < S-dA₃₆.

Table 1: Summary of the $\log[K\omega_{\text{app}}]/\log[\text{NaCl}]$ Dependence, and Experimental and Calculated $K\omega_{\text{app}}$ Values, for Complexes of Wild-Type Gene 5 Protein and Different dA₃₆ Oligonucleotides (0.2 M NaCl, 20 °C)^{a,b}

sequence	slope ^c $-\log[K\omega_{\text{app}}]/\log[\text{NaCl}]$	experimental $K\omega_{\text{app}}$ ($\times 10^{-5} \text{ M}^{-1}$)	calculated $K\omega_{\text{app}}$ ($\times 10^{-5} \text{ M}^{-1}$) ^d	
			zeroth-neighbor	nearest-neighbor
P-dA ₃₆	3.68 ± 0.29	0.71 ± 0.05	0.61 ± 0.04	0.70 ± 0.10
SSSP-dA ₃₆	3.32 ± 0.49	1.69 ± 0.25	2.66 ± 0.14	2.15 ± 0.18
SSPP-dA ₃₆	3.29 ± 0.34	10.3 ± 0.82	11.6 ± 0.55	9.33 ± 0.43
(S ₃ ,P)-dA ₃₆	2.85 ± 0.61	35.0 ± 6.8	49.1 ± 2.9	40.5 ± 2.2
S-dA ₃₆	2.70 ± 0.28	246 ± 21	220 ± 17	249 ± 17

^a Experimental data were extrapolated to 0.2 M NaCl. ^b Titration endpoints were all at $[\text{P}]/[\text{N}] = 0.25\text{--}0.26 \pm 0.01$, with standard deviations determined by fitting CD titration data at 270 nm with two linear regressions. ^c Slope and standard deviations from linear regressions of the data in Figure 3B. ^d Zeroth-neighbor and nearest-neighbor values are from singular value decompositions and with standard deviations derived as described in the text.

As in previous work (26), the measured dissociation data were compared with calculated curves based on two finite-lattice binding models, the all-or-none and the one-cluster models. In the all-or-none model, two 36-mer strands are assumed either to be saturated by nine g5p dimers or to have no bound proteins. For the highly cooperative g5p, calculated curves based on the all-or-none model were in good agreement with the measured dissociation data for all five types of complexes, as shown in Figure 3A. Curves calculated for the one-cluster model, based on the assumption that dissociation occurred from the ends of one cluster of protein on each lattice, did not agree with the measured dissociation data (data not shown).

Binding Affinities to P-dA₃₆ and S-dA₃₆. Complexes with each oligomer were formed at four different protein concentrations and were salt-dissociated. Dissociation data for each complex were fitted with a function as described in Mou et al. (26) to determine the NaCl concentrations at 50% dissociation. Then, the binding affinities ($K\omega_{\text{app}}$) were determined from the free protein dimer concentrations (L) at 50% dissociation for each complex [$K\omega_{\text{app}} = 1/(2L)$; see Materials and Methods]. $K\omega_{\text{app}}$ values are plotted as a function of NaCl concentration on a log–log scale in Figure 3B. Figure 3B shows that the logarithm of the binding affinity, $\log[K\omega_{\text{app}}]$, was linearly related to the logarithm of the salt concentration, $\log[\text{NaCl}]$, for each complex. The slopes of the $\log[K\omega_{\text{app}}]$ versus $\log[\text{NaCl}]$ plots are listed in Table 1. The slope of -3.7 ± 0.3 for binding to P-dA₃₆ was comparable to the slope of -3.2 ± 0.4 for binding to P-dA₄₈ (26), but was 20% less than that for binding to poly[d(A)] (32, 39). The slopes give the number of ions released per protein dimer when forming a complex (32). These ranged from 3.7 to 2.7 and decreased as the proportion of phosphorothioate linkages increased. Only about three ions were released per g5p dimer when binding to S-dA₃₆, approximately one ion less than when binding to P-dA₃₆.

The experimental $K\omega_{\text{app}}$ values for binding to the five oligodeoxyadenylic acids were significantly different and varied by over 2 orders of magnitude when extrapolated to the same salt concentration of either 0.2 M NaCl (Table 1) or 1.0 M NaCl (not shown). The value of $K\omega_{\text{app}}$ for binding to S-dA₃₆ was >300-fold higher than for binding to P-dA₃₆, and binding affinities increased in the order of P-dA₃₆ < SPPP-dA₃₆ < SSPP-dA₃₆ < (S₃,P)-dA₃₆ < S-dA₃₆. The $K\omega_{\text{app}}$ value of $0.71 \times 10^5 \text{ M}^{-1}$ at 0.2 M NaCl for P-dA₃₆ was less than values of 1.10×10^5 and $1.61 \times 10^5 \text{ M}^{-1}$ for P-dA₄₈ and poly[dA], respectively, at the same salt concentration (25, 26). This was expected because of the reduced number

of cooperative interactions. One can use the $K\omega_{\text{oligo}}$, observed for binding to a 36-mer, to calculate the ω_{pol} for binding to a polymer. In particular, the cooperativity factor ω_{pol} can be calculated from the ratio of the binding affinity of m dimers in the midst of a polymer lattice to the binding affinity to an oligomer lattice; the formula is $\omega_{\text{pol}} = (K\omega_{\text{pol}}/K\omega_{\text{oligo}})^m$ (26). For binding of nine dimers to the 36-mer, ω_{pol} is estimated to be 1600. This is in the range of values of 500–5000 reported by Bultink et al. (39) and Terwilliger (32).

To help determine the origin of the relative binding affinities of g5p to these dA₃₆ oligonucleotides, the data were fitted by the zeroth-neighbor model (which depends on two parameters that characterize the P and S linkage composition) and the nearest-neighbor model (which depends on three parameters that characterize neighboring linkages) as described in Materials and Methods. Singular value decomposition (SVD) was used to obtain a simultaneous fit to the $\log[K\omega_{\text{app}}]$ data from all five sequences for each model. The fits to the $\log[K\omega_{\text{app}}]$ data according to zeroth-neighbor (dashed line) and nearest-neighbor (solid line) models are plotted in Figure 3B. SVD-calculated values that were extrapolated to 0.2 M NaCl are tabulated in the last two columns of Table 1.

A statistical test of the models was by the Q probability; a larger Q value indicates a better fit (see Materials and Methods). Q probabilities were 0.0001 and 0.29 for fits of the data to the zeroth-neighbor and nearest-neighbor models, respectively. The agreement was significant for the nearest-neighbor model, but the data were not quite accounted for by the two zeroth-neighbor parameters. Nevertheless, the binding affinities were dominated by the simple phosphorothioate contents of the d(A)₃₆ oligomers. This may be seen in Figure 3B and by comparing the experimental and zeroth-neighbor calculated values in Table 1. These latter values are plotted in Figure 4, which shows $\log[K\omega_{\text{app}}]$ at 0.2 M NaCl as a function of phosphorothioate content. The deviations of the experimental values from the straight line (zeroth-neighbor) dependence illustrate the magnitude of a small nearest-neighbor effect that slightly reduced the relative binding affinity of a phosphorothioate linkage when it occurred adjacent to a phosphodiester linkage.

Binding Affinities to P-d(AAC)₁₂ and S-d(AAC)₁₂. To investigate whether base stacking could influence the binding to S-DNAs, the binding affinities of g5p were determined for two 36-mers, P-d(AAC)₁₂ and S-d(AAC)₁₂. These contained d(AC) + d(CA) neighbors that were shown in previous work to be less stacked than d(AA) neighbors and that bound g5p with higher affinity (26). First, protein

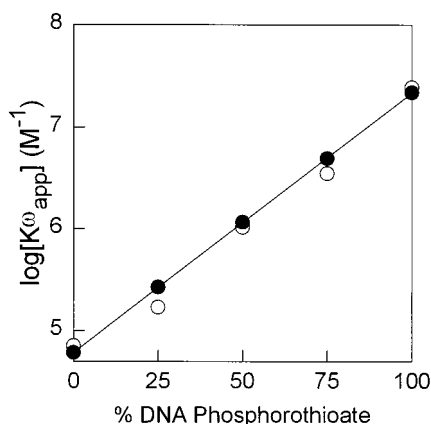


FIGURE 4: Fit of two parameters from the zeroth-neighbor model to the binding affinities of g5p for sequences of different phosphorothioate contents. The experimental $\log[Kw_{app}]$ values (○) and the SVD-calculated $\log[Kw_{app}]$ values for the zeroth-neighbor model (●) at 0.2 M NaCl are from the data in Table 1. The fit shows that the experimental $\log[Kw_{app}]$ values were dominated by the two zeroth-neighbor parameters, which describe the effect of changing the composition of phosphorothioate linkages in the sequences. Differences between the experimental data and the zeroth-neighbor calculated values were consistent with a small effect of nearest-neighbor interactions.

Table 2: Summary of the $\log[Kw_{app}]/\log[NaCl]$ Dependence and Kw_{app} Values for Complexes of Wild-Type Gene 5 Protein with P-d(AAC)₁₂ or S-d(AAC)₁₂ and Complexes of Wild-Type and Mutant Gene 5 Proteins with P-dA₃₆ or S-dA₃₆ (0.2 M NaCl, 20 °C)^{a,b}

protein in complex	sequence in complex	slope ^c — $\log[Kw_{app}]/\log[NaCl]$	experimental Kw_{app} ($\times 10^{-5} M^{-1}$)
wild-type	P-d(AAC) ₁₂	3.05 ± 0.07	19.3 ± 0.01
wild-type	S-d(AAC) ₁₂	nd ^d	$> 1000^e$
wild-type	P-dA ₃₆	3.68 ± 0.29	0.71 ± 0.05
Y26F	P-dA ₃₆	4.01 ± 0.48	0.20 ± 0.01
Y34F	P-dA ₃₆	3.65 ± 0.25	0.060 ± 0.002
Y61F	P-dA ₃₆	3.91 ± 0.69	0.40 ± 0.04
wild-type	S-dA ₃₆	2.70 ± 0.28	246 ± 21
Y26F	S-dA ₃₆	2.61 ± 0.47	86.9 ± 2.1
Y34F	S-dA ₃₆	2.53 ± 0.16	33.4 ± 0.8
Y61F	S-dA ₃₆	2.77 ± 1.07	206 ± 29.4

^a Experimental data were extrapolated to 0.2 M NaCl. ^b Titration endpoints were all at $[P]/[N] = 0.25-0.26 \pm 0.01$, with standard deviations determined by fitting CD titration data at 270 nm with two linear regressions. ^c Slope and standard deviation from linear regressions of the data in Figure 3B and Supporting Information Figure S1. ^d Not determined. ^e The calculated value was $(6690 \pm 1320) \times 10^5 M^{-1}$. See legend to Figure 5.

titrations confirmed that the binding stoichiometry was the expected four nucleotides per g5p monomer for both d(AAC)₁₂ and S-d(AAC)₁₂ (Table 2 footnote). Then, samples were subjected to salt dissociations to determine Kw_{app} values as described above for the other 36-mers. Figure 5 shows the $[NaCl]$ -dependence of the measured values of $\log[Kw_{app}]$ of g5p for P-d(AAC)₁₂, P-dA₃₆, and S-dA₃₆. The binding affinity was 27-fold higher for P-d(AAC)₁₂ than for P-dA₃₆ at 0.2 M NaCl (Table 2). Reliable salt dissociation curves could not be determined for complexes with S-d(AAC)₁₂ because of incomplete dissociation and precipitation of protein at high $[NaCl]$. But, the NaCl concentrations required for dissociation of complexes with S-d(AAC)₁₂ were within the shaded area of Figure 5 and were at least as great as

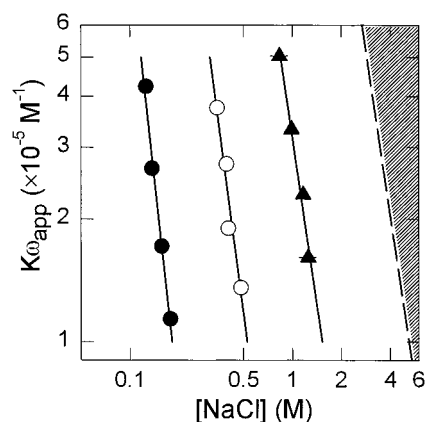


FIGURE 5: Effect on g5p binding affinity of changing both the backbone and the nearest-neighbor base composition in DNA. Values for $\log[Kw_{app}]$ versus $\log[NaCl]$ plots were obtained by salt-dissociation of complexes formed with P-dA₃₆ (●), P-d(AAC)₁₂ (○), or S-dA₃₆ (▲) at a $[P]/[N]$ ratio of 0.25. The predicted binding affinity for S-d(AAC)₁₂ is shown as a dashed line (— —). The slope of the $\log[Kw_{app}]/\log[NaCl]$ for S-d(AAC)₁₂ was assumed to be the same as for S-dA₃₆, and the Kw_{app} value for S-d(AAC)₁₂ at 0.2 M NaCl was derived from the experimental Kw_{app} values for the other three complexes at the same NaCl concentration according to the equation $\log[Kw_{app}]_{S-dAAC} = \log[Kw_{app}]_{S-dA} + \log[Kw_{app}]_{P-dAAC} - \log[Kw_{app}]_{P-dA}$. Precise experimental dissociation data for g5p·S-d(AAC)₁₂ complexes could not be obtained because of the high salt concentrations needed for dissociation, but the $[NaCl]$ values for two samples were within the upper portion of the shaded area and indicated a significant additional influence of the nearest-neighbor base stacking effect on the binding affinity for S-d(AAC)₁₂. Error bars were within the size of the symbols shown.

would be predicted by adding the free energy contribution of the d(AC) + d(CA) nearest neighbors in normal P-DNA to the contribution of the phosphorothioation of dA₃₆ (see legend to Figure 5). Therefore, it appeared that there was a significant nearest-neighbor d(AA) base-stacking effect on the binding affinity of g5p to the phosphorothioate-containing dA₃₆ sequences.

Binding Affinities of Mutant Gene 5 Proteins. The g5p contains five conserved tyrosines, and four mutant proteins with conservative Tyr → Phe substitutions have been characterized in prior work (28, 29). Tyr-26, Tyr-34, and Tyr-61 are assigned as being involved in DNA binding, protein–protein cooperative interactions, and protein folding, respectively. Mutant proteins Y26F, Y34F, and Y61F all have reduced binding affinity for ssDNA compared with the wild-type protein (29). In the present work, the $\log[Kw_{app}]$ versus $\log[NaCl]$ dependence was determined for the binding of each of these mutants to P-dA₃₆ and S-dA₃₆. The affinities for P-dA₃₆ were in the order of wild-type > Y61F > Y26F > Y34F (with relative values of $1 > 0.56 \pm 0.07 > 0.28 \pm 0.02 > 0.08 \pm 0.01$) when extrapolated to a salt concentration of 0.2 M NaCl. (Data are summarized in Table 2, and the $\log[Kw_{app}]$ versus $\log[NaCl]$ plots are given in Figure S1 of Supporting Information.) At the same salt concentration, the affinities for S-dA₃₆ were in the same order with relative values of $1 > 0.84 \pm 0.14 > 0.35 \pm 0.03 > 0.14 \pm 0.01$. The data are summarized in Table 2. Since the general effects of the three mutations were the same regardless of the type of DNA substrate, these results support the other evidence above that the phosphorothioate DNA binds in the normal g5p binding site. Further, the ratios for binding of the mutants

to the phosphorothioate DNA were slightly higher than for binding to the normal DNA, indicating that the binding affinities of the mutants, relative to that of the wild-type protein, were reduced slightly less when the substrate was the modified DNA. That is, the higher affinity to the S-dA₃₆ may modestly compensate for the destabilizing effects of these mutations. Finally, the slopes of the plots for binding to S-dA₃₆ were all slightly less than for binding to P-dA₃₆ by about one ion per protein dimer, regardless of the protein used. Values of the slopes are given in Table 2. This reinforced the conclusion from titrations with the wild-type protein (Table 1) that a reduction in the number of ions released was a property of DNA backbone phosphorothioation.

DISCUSSION

S-dA₃₆ Binds in the Normal g5p Binding Site. The phosphorothioate-modified and unmodified dA₃₆ oligomers were similar in (A) having identical stoichiometries of binding (e.g., binding in an $n = 4$ nucleotide/protein monomer mode), (B) giving the same qualitative CD changes on binding, (C) being dissociated in the same all-or-none fashion by salt, and (D) having the same ranking of binding affinities for three mutant proteins. We are led to the conclusion that phosphorothioate-modified and unmodified dA₃₆ oligomers bind to the same binding site of Ff gene 5 protein.

The K_w for binding to a g5p dimer was about 350-fold greater for S-d(A)₃₆ than for P-d(A)₃₆ at 0.2 M NaCl (Table 1), with the assumption that the data in Figure 3B may be linearly extrapolated to this salt concentration. (Confidence in the reasonableness of a linear extrapolation is provided by the similar slopes for the $\log[K_w]$ versus $\log[\text{NaCl}]$ plots that describe the binding of the wild-type and three mutant g5p proteins to a particular oligomer over a wide range of NaCl concentrations, Table 2 and Supporting Figure S1.) At 20 °C and 0.2 M NaCl, the free energy of binding per phosphorothioate linkage was more favorable by about 0.4 kcal/mol ($\Delta G^\circ = -[RT \ln(350)]/8$). The binding affinity increased in a nearly linear fashion with the extent of phosphorothioation. In addition, SPPP-dA₃₆ and SSPP-dA₃₆, which had modifications that presumably would have been phased in the g5p binding site in an $n = 4$ binding mode, were not disproportionate in their binding affinities. Therefore, the higher binding affinity of phosphorothioate linkages to g5p was not dominated by one or two position-specific interactions between sulfur and protein residues.

Enhanced Binding of S-DNA by g5p Is Not a Polyelectrolyte Effect. Polyelectrolyte contributions are a major source of stability in DNA-protein interactions (40). However, the number of ions released upon binding was about one less per g5p dimer for binding of S-d(A)₃₆ than for binding of P-d(A)₃₆ (see values of slopes in Tables 1 and 2). This reduction in ion release due to phosphorothioate-modification could be caused, in part, by a slight unstacking in S-d(A)₃₆ versus P-d(A)₃₆ (see below) and a consequent increase in the phosphate-phosphate distance and reduction in charge density. Fewer ions released contributed to an unfavorable entropy of binding for S-d(A)₃₆. Moreover, with the assumption that preferential ion binding effects are small and that $\log(K_w)$ values may be extrapolated and compared at 1 M

NaCl where the polyelectrolyte effect is eliminated (40), the differences in binding affinities of S-d(A)₃₆ versus P-d(A)₃₆ due to nonpolyelectrolyte effects were actually somewhat larger than those tabulated at 0.2 M NaCl in Table 1. That is, the enhanced binding of phosphorothioate DNA resided in factors such as altered DNA structure, electrostatic (ionic) interactions, and nonelectrostatic interactions.

Effects of Altered S-DNA Structure. The phosphorothioate could affect binding affinity by changes in the nucleic acid flexibility and base-base stacking (41–43). White et al. (44) showed by IR spectra that S-DNA and P-DNA have significant structural differences at all relative humidities.

(A) The water bound in the first layer of hydration is slightly less for a 20-mer pyrimidine-rich S-DNA than for the unmodified DNA (1.2 versus 1.4 water molecules/nucleotide absorbed over the water bound at 0% RH) (44). Therefore, the entropic contribution of water release (at least from the nucleic acid) should be no more favorable for S-DNA than for P-DNA.

(B) Increased steric hindrance of phosphorothioate DNA caused by the larger radius of the sulfur (1.8 Å) compared with oxygen (1.5 Å) could reduce the entropic cost of binding of phosphorothioates to proteins, as was pointed out by Benimetskaya et al. (45). However, such a reduction should be minimal in the case of S-d(A)₃₆ binding to g5p. First, the phosphorothioate linkage, while having a preferred conformation, is still flexible (41). Adenine stacking constrains the conformations of both P-d(A)₃₆ and S-d(A)₃₆, and a slight unstacking of bases in S-d(A)₃₆ (following paragraph) might actually increase its flexibility relative to P-d(A)₃₆. Second, the sign of an entropic effect depends on the bound as well as the free state of the nucleic acid (including changes in the water of hydration). For example, in previous work we found that entropy changes were favorable for hybridization of S-DNAs with RNAs (by about +1.7 cal/mol of base pair) but were unfavorable for hybridization of S-DNAs to form S-DNA•DNA or S-DNA•S-DNA duplexes (by about –3.3 cal/mol of base pair), relative to P-DNA hybridization (46). In the case of binding to g5p, it seems unlikely that S-d(A)₃₆ would be less constrained than P-d(A)₃₆ in left-handed helical channels when saturated by g5p, although their local nucleotide conformations may differ.

(C) Steric hindrance or electrostatic effects of the sulfur (41–43, 47) that reduce the interaction between neighboring bases could lead to a favorable enthalpy of binding. G5p binds to unstacked sequences with much higher affinity than to stacked sequences (26). Differences in the binding affinity of g5p for normal DNA sequences are consistent with a nearest-neighbor nucleotide effect in which a reduction in base–base stacking in the free nucleic acid results in a net gain in enthalpy as the bases stack with aromatic residues (Phe-73 and Tyr-26) in the g5p binding site and as bases partially restack with themselves within the overall left-handed superhelix complex. A negative CD band of dA₃₆ at 250 nm, an indication of base-base interaction (48), was about one-third reduced for S-dA₃₆ compared with P-dA₃₆ (see the solid lines for free P-dA₃₆ and S-dA₃₆ in Figure 1, panels A and B); this CD band was intermediate in magnitude for the other S-containing oligomers. The hyperchromicity at 260 nm upon heating from 20 to 90 °C was also slightly reduced from 22% (for P-dA₃₆) to 18% (for S-dA₃₆; data not shown). Therefore, S-dA₃₆ appeared to be

slightly unstacked, consistent with previous results for other phosphorothioate-modified DNA sequences (46). But, other results argue against S-DNA unstacking as dominating its higher binding affinity. For the S-DNA oligomers, the reduced change in the CD band at 270 nm during complex formation (Figure 2) suggests that base-amino acid stacking was reduced and/or other local features of the bound S-dA₃₆ were not like those of bound P-dA₃₆. If reduced stacking of S-dA₃₆ bases made them more accessible for interactions with the protein, one might have expected the same, or an enhanced, change in the CD on binding. Of more importance, base unstacking caused by phosphorothioate substitution did not appreciably reduce the unstacking effect caused by substitution of purine–purine neighbors with purine–pyrimidine neighbors, because the binding affinity of S-d(AAC)₁₂ was significantly increased over that of S-d(A)₃₆ (Figure 5). In summary, although conformational perturbations of the DNA due to phosphorothioation undoubtedly modulated the binding affinity of g5p to S-d(A)₃₆ compared with P-d(A)₃₆, direct interactions of the phosphorothioate group with the protein were the more likely contributors to the net higher binding affinity of S-d(A)₃₆.

Direct Effects of Sulfur. Sulfur is less electronegative than oxygen, but the sulfur probably carries a full negative charge in phosphorothioate anions in solution because the larger size and polarizability of sulfur allow the charge density in a thiolate anion to be less than that in an oxyanion (41, 49). The net effect on the properties of phosphorothioate DNA is difficult to predict.

Dertinger et al. (50) used a phosphorothioate walk with single, chiral-specific substitutions along an RNA hairpin to study the effects of individual phosphorothioate substitutions on binding of the MS2 virus coat protein. They found that the direct, specific effects of phosphorothioate substitutions could be either positive or negative, in the range of 0.4–1.6 kcal/mol, without an obvious correlation between the size of the effect and the type of interaction (hydrogen bonding or ionic).

In the present work, the phosphorothioate substitutions were of random chirality, requiring that a mixture of nonsite-specific interactions between the g5p and the individual substituted backbone linkages netted a favorable binding. Contributions to the binding energy could include (A) reinforcement of electrostatic effects (42, 43, 47), (B) a contribution from stacking interactions with sulfur, which is more polarizable than oxygen (51), (C) an increased hydrophobic effect (52, 53), and (D) a smaller enthalpy required to strip water and ions from the S-DNA backbone (54).

SUPPORTING INFORMATION AVAILABLE

One figure showing the dependence of log[*K*ω] on log-[NaCl] for binding of different g5p mutants to dA₃₆ and S-dA₃₆. This material is available free of charge via the Internet at <http://pubs.acs.org>.

REFERENCES

- Stein, C. A., Subasinghe, C., Shinozuka, K., and Cohen, J. S. (1988) *Nucleic Acids Res.* 16, 3209–3221.
- Ho, P. T., Ishiguro, K., Wickstrom, E., and Sartorelli, A. C. (1991) *Antisense Res. Dev.* 1, 329–342.
- Zhao, Q., Matson, S., Herrera, C. J., Fisher, E., Yu, H., and Krieg, A. M. (1993) *Antisense Res. Dev.* 3, 53–66.
- Ghosh, M. K., Ghosh, K., and Cohen, J. S. (1993) *Anti-cancer Drug Des.* 8, 15–32.
- Yakubov, L., Khaled, Z., Zhang, L. M., Truneh, A., Vlassov, V., and Stein, C. A. (1993) *J. Biol. Chem.* 268, 18818–18823.
- Bergan, R. C., Kyle, E., Connell, Y., and Neckers, L. (1995) *Antisense Res. Dev.* 5, 33–38.
- Guvakova, M. A., Yakubov, L. A., Vlodavsky, I., and Stein, C. A. (1995) *J. Biol. Chem.* 270, 2620–2627.
- Weidner, D. A., Valdez, B. C., Henning, D., Greenberg, S., and Busch, H. (1995) *FEBS Lett.* 366, 146–150.
- Cheng, X., DeLong, R. K., Wickstrom, E., Kligshsteyn, M., Demirdji, S. H., Caruthers, M. H., and Juliano, R. L. (1997) *J. Mol. Recognit.* 10, 101–107.
- Matthes, E., and Lehmann, Ch. (1999) *Nucleic Acids Res.* 27, 1152–1158.
- Brunker, I., and Tremblay, G. A. (2000) *Biochemistry* 39, 11463–11466.
- Skinner, M. M., Zhang, H., Leshnitzer, D. H., Guan, Y., Bellamy, H., Sweet, R. M., Gray, C. W., Konings, R. N. H., Wang, A. H.-J., and Terwilliger, T. C. (1994) *Proc. Natl. Acad. Sci. U.S.A.* 91, 2071–2075.
- Folkers, P. J., Nilges, M., Folmer, R. H., Konings, R. N., and Hilbers, C. W. (1994) *J. Mol. Biol.* 236, 229–246.
- Gray, C. W. (1989) *J. Mol. Biol.* 208, 57–64.
- Folmer, R. H. A., Nilges, M., Folkers, P. J. M., Konings, R. N. H., and Hilbers, C. W. (1994) *J. Mol. Biol.* 240, 341–357.
- Guan, Y., Zhang, H., and Wang, A. H.-J. (1995) *Protein Sci.* 4, 187–197.
- Olah, G. A., Gray, D. M., Gray, C. W., Kergil, D. L., Sosnick, T. R., Mark, B. L., Vaughan, M. R., and Trehwella, J. (1995) *J. Mol. Biol.* 249, 576–594.
- King, G. C., and Coleman, J. E. (1988) *Biochemistry* 27, 6947–6953.
- Shamoo, Y., Friedman, A. M., Parsons, M. R., Konigsberg, W. H., and Steitz, T. A. (1995) *Nature* 376, 362–366.
- Bochkarev, A., Pfuetzner, R. A., Edwards, A. M., and Frappier, L. (1997) *Nature* 385, 176–181.
- Alma, N. C. M., Harmsen, B. J. M., van Boom, J. H., van der Marel, G., and Hilbers, C. W. (1983) *Biochemistry* 22, 2104–2115.
- Folkers, P. J. M., van Duynhoven, J. P. M., van Lieshout, H. T. M., Harmsen, B. J. M., van Boom, J. H., Tesser, G. I., Konings, R. N. H., and Hilbers, C. W. (1993) *Biochemistry* 32, 9407–9416.
- Dick, L. R., Gerald, C. F. G. C., Sherry, A. D., Gray, C. W., and Gray, D. M. (1988) *Biochemistry* 28, 7896–7904.
- Dick, L. R., Sherry, A. D., Newkirk, M. M., and Gray, D. M. (1989) *J. Biol. Chem.* 263, 18864–18872.
- Sang, B.-C., and Gray, D. M. (1989) *J. Biomol. Struct. Dyn.* 7, 693–706.
- Mou, T.-C., Gray, C. W., and Gray, D. M. (1999) *Biophys. J.* 76, 1537–1551.
- Terwilliger, T. C., Zabin, H. B., Horvath, M. P., Sanberg, W. S., and Schlunk, P. M. (1994) *J. Mol. Biol.* 236, 556–571.
- Mark, B. L., Terwilliger, T. C., Vaughan, M. R., and Gray, D. M. (1995) *Biochemistry* 34, 12854–12865.
- Thompson, T. M., Mark, B. L., Gray, C. W., Terwilliger, T. C., Sreerama, N., Woody, R. W., and Gray, D. M. (1998) *Biochemistry* 37, 7463–7477.
- Gray, D. M., Hung, S.-H., and Johnson, K. H. (1995) *Methods Enzymol.* 246, 19–34.
- Murphy, J. H., and Trapane, T. L. (1996) *Anal. Biochem.* 240, 273–282.
- Terwilliger, T. C. (1996) *Biochemistry* 35, 16652–16664.
- McGhee, J. D., and von Hippel, P. H. (1974) *J. Mol. Biol.* 86, 469–489.
- Gray, D. M. (1997) *Biopolymers* 42, 783–793.
- Press, W. H., Turkolosky, S. A., Vetterling, W. T., and Flannery, B. P. (1992) *Numerical Recipes in C*, 2nd ed., pp 59–70, Cambridge University Press, New York.
- Gray, D. M. (1997) *Biopolymers* 42, 795–810.

37. Antao, V. P., and Gray, D. M. (1993) *J. Biomol. Struct. Dyn.* 10, 819–839.
38. Gray, D. M. (1996) in *Circular Dichroism and the Conformational Analysis of Biomolecules* (Fasman, G. D., Ed.) pp 469–500, Plenum Press, New York.
39. Bulsink, H., Harmsen, B. J., and Hilbers, C. W. (1985) *J. Biomol. Struct. Dyn.* 3, 227–247.
40. Lohman, T. M., and Mascotti, D. P. (1992) *Methods Enzymol.* 212, 400–424.
41. Florián, J., Strajbl, M., and Warshel, A. (1998) *J. Am. Chem. Soc.* 120, 7959–7966.
42. Smith, J. S., and Nikonowicz, E. P. (2000) *Biochemistry* 39, 5642–5652.
43. Johansson, H. E., Dertinger, D., LeCuyer, K. A., Behlen, L. S., Greef, C. H., and Uhlenbeck, O. C. (1998) *Proc. Natl. Acad. Sci. U.S.A.* 95, 9244–9249.
44. White, A. P., Reeves, K. K., Snyder, E., Farrell, J., Powell, J. W., Mohan, V., Griffey, R. H., and Sasmor, H. (1996) *Nucleic Acids Res.* 24, 3261–3266.
45. Benimetskaya, L., Tonkinson, J. L., Koziolkiewicz, M., Karwowski, B., Guga, P., Zelster, R., Stec, W., and Stein, C. A. (1995) *Nucleic Acids Res.* 23, 4239–4245.
46. Clark, C. L., Cecil, P. K., Singh, D., and Gray, D. M. (1997) *Nucleic Acids Res.* 25, 4098–4105.
47. Hartmann, B., Bertand, H.-O., and Femandjian, S. (1999) *Nucleic Acids Res.* 27, 3342–3347.
48. Greve, J., Maestre, M. F., Moise, H., and Hosoda, J. (1978) *Biochemistry* 17, 887–893.
49. Frey, P. A., and Sammons, R. D. (1985) *Science* 228, 541–545.
50. Dertinger, D., Behlen, L. S., and Uhlenbeck, O. C. (2000) *Biochemistry* 39, 55–63.
51. Saenger, W. (1984) *Principles of Nucleic Acid Structure*, pp 117, 185, Springer-Verlag, NY.
52. Ha, J. H., Spolar, R. S., and Record, M. T. Jr. (1989) *J. Mol. Biol.* 209, 801–816.
53. Spolar, R. S., and Record, M. T., Jr. (1994) *Science* 263, 777–784.
54. Cho, Y. S., Zhu, F. C., Luxon, B. A., and Gorenstein, D. G. (1993) *J. Biomol. Struct. Dyn.* 11, 685–702.

BI002136F